Excited-State Charge Transfer Dynamics of *p*-Dimethylaminobenzonitrile in Quadrupolar Solvents†

Sudha Dorairaj and Hyung J. Kim*
Department of Chemistry, Carnegie Mellon University, 4400 Fifth Ave, Pittsburgh, Pennsylvania 15213-2683

Received: August 2, 2001; In Final Form: December 18, 2001

Excited-state intramolecular charge transfer of *p*-dimethylaminobenzonitrile (DMABN) in benzene, toluene, and dioxane is studied. By combining the recent continuum quadrupolar solvent theory of Jeon and Kim [*J. Phys. Chem. A* **2000**, *104*, 9812] and the two-dimensional formulation of the DMABN photoreaction in dipolar solvents by Fonseca et al. [*J. Mol. Liq.* **1994**, *60*, 161], the influence of both solvent quadrupole reorganization and solute twist on the reaction free energetics and dynamics is accounted for. The solution-phase reaction paths are investigated with the aid of experimental information on the frequencies associated with solute torsional and collective solvent quadrupole dynamics. The rate constants and transmission coefficients are analyzed using transition state theory with the neglect of dissipative dynamics. Our results are in reasonable agreement with the experimental findings in quadrupolar solvents.

1. Introduction

Since dual fluorescence of *p*-dimethylaminobenzonitrile (DMABN) was first observed in solution four decades ago,[1] a great deal of attention has been paid to its excited-state intramolecular charge transfer (EICT) dynamics.[2−23] Though it is still controversial to some extent,[13,17] the twisted intramolecular charge transfer (TICT) idea proposed more than twenty years ago[2] provides an excellent mechanistic framework to understand and interpret photoreactions of DMABN and related molecules. In this TICT picture, EICT from the reactant state, which is initially in a planar geometry on the S_1 electronic surface of DMABN, is accompanied by twisting of the dimethylamino group with respect to the phenyl ring, so that the two moieties become perpendicular in the product state. As evidenced by many experimental findings that DMABN photoreactions occur in solution and not in a vacuum, solvation plays a crucial role in this reaction class.

A previous analysis of EICT kinetics by Kim and Hynes[18] using a non-Markovian description couched in the two-dimensional reaction coordinate formulation[14] to account for the DMABN twist and solvent polarization dynamics has yielded good agreement with measurements[19,20] in acetonitrile and alcohols. One of the noteworthy findings there is that in highly polar solvents, the twist angle θ between the dimethylamino group and phenyl ring is $\sim 25°-30°$ at the transition state. Thus DMABN does not need to undergo a full 90° twist before charge transfer can occur; a rearrangement of relatively small amplitude in θ (this, of course, needs to be accompanied by necessary solvent reorganization) is sufficient for the system to reach the transition state.[14] This is in line with its rapid EICT kinetics observed in acetonitrile and small alcohols. This early transition in highly polar solvents arises from strong solvation stabilization of the charge-transfer product state, which tends to make the transition state more like the planar reactant state ("Hammond postulate").[14]

While EICT for DMABN and closely associated derivatives occurs mainly in solvents of high polarity, it is observed also in nondipolar or weakly dipolar solvents with large molecular quadrupole moments, such as benzene, toluene, and dioxane.[13] Hereafter, these will be referred to as quadrupolar solvents.[24] This indicates that there exists significant outer-sphere reorganization in this solvent class, just like in highly dipolar solvents. Several other experiments on electron transfer[25−29] and solvation dynamics[30−32] lend further support to the importance of solvent quadrupole reorganization. However, there have been only limited theoretical efforts to understand and quantify the solvation effects on charge shift and transfer processes in quadrupolar solvents.[33,34,29] Recently, Jeon and Kim have developed a continuum theory to describe equilibrium and nonequilibrium solvation in quadrupolar solvents.[35,36] Its application[37] to electron-transfer free energetics in benzene has yielded reasonable agreement with experiments.[28,29] In this paper, we extend this theory to include collective solvent quadrupole dynamics and apply it to study the DMABN photoreactions in benzene, toluene, and dioxane.[24] As noted in section 3 below, with minor changes, the formal structure of the TICT description we derive in the quadrupolar solvents becomes identical to that of related previous studies in the dipolar solvents.[14,18] Thus, we will extensively utilize this connection to the earlier analyses[14,18] and present only the main results in the current contribution. For technical details, the reader is referred to refs 14 and 18.

The outline of this paper is as follows. In section 2, we give a brief review of the continuum theory of quadrupolar solvents.[35−37] The two-state electronic description used for excited-state DMABN and two-dimensional reaction coordinate formulation of its EICT are explained in section 3. The results on the reaction free energy surfaces, reaction paths, and rate constants in benzene, toluene, and dioxane are presented in section 4, while section 5 concludes.

2. Continuum Theory of Quadrupolar Solvents

We begin with a brief reprise of the recent continuum formulation of equilibrium and nonequilibrium solvation in a polarizable and quadrupolar solvent by Jeon and Kim.[35−37] The solvent is described in terms of the densities of its quadrupole and induced dipole moments; hereafter, these densities will be referred to as quadrupolarization and electronic polarization

† Part of the special issue "Noboru Mataga Festschrift".
* Corresponding author.

10.1021/jp012991o CCC: $22.00
Published on Web 02/16/2002

fields, $\mathbf{Q}$ and $\mathbf{P}_{el}$, respectively. For a solute immersed in a cavity that excludes the solvent, the total Hamiltonian $\hat{H}$ in the presence of arbitrary $\mathbf{P}_{el}$ and $\mathbf{Q}$ is[35,36]

$$\hat{H} = \hat{H}^0 + \frac{1}{2\chi_{el}}\int^V d\mathbf{r}\,|\mathbf{P}_{el}(\mathbf{r})|^2 + \frac{1}{2}\int^V d\mathbf{r}\int^V d\mathbf{r}'\,\mathbf{P}_{el}(\mathbf{r})\cdot\left[\vec{\nabla}\vec{\nabla}'\frac{1}{|\mathbf{r}-\mathbf{r}'|}\right]\cdot\mathbf{P}_{el}(\mathbf{r}') - \int^V d\mathbf{r}\,\mathbf{P}_{el}(\mathbf{r})\cdot\hat{\mathcal{E}}(\mathbf{r}) + \frac{1}{6C_Q}\int^V d\mathbf{r}\,\mathbf{Q}(\mathbf{r}):\mathbf{Q}(\mathbf{r}) + \frac{1}{3}\int^V d\mathbf{r}\int^V d\mathbf{r}'\,\mathbf{P}_{el}(\mathbf{r})\cdot\left[\vec{\nabla}\vec{\nabla}'\vec{\nabla}'\frac{1}{|\mathbf{r}-\mathbf{r}'|}\right]:\mathbf{Q}(\mathbf{r}') + \frac{1}{18}\int^V d\mathbf{r}\int_{0+}^V d\mathbf{r}'\,\mathbf{Q}(\mathbf{r}):\left[\vec{\nabla}\vec{\nabla}\vec{\nabla}'\vec{\nabla}'\frac{1}{|\mathbf{r}-\mathbf{r}'|}\right]:\mathbf{Q}(\mathbf{r}') - \frac{1}{3}\int^V d\mathbf{r}\,\mathbf{Q}(\mathbf{r}):\vec{\nabla}\hat{\mathcal{E}} \quad (1)$$

where $\hat{H}^0$ and $\hat{\mathcal{E}}$ are the solute electronic Hamiltonian and electric field operators in a vacuum, $\mathbf{r}$ and $\mathbf{r}'$ represent positions in the solvent medium, the superscript V indicates that the integrations are restricted to the volume outside the cavity, and A:B for second-rank tensors $\mathbf{A}$ and $\mathbf{B}$ denotes $\sum_{i,j} A_{ij}B_{ij}$. For simplicity, both the dipolar and quadrupolar susceptibilities, χ_{el} and C_Q, are assumed to be scalars. The former is related to the optical dielectric constant $\epsilon_\infty = 1 + 4\pi\chi_{el}$. In eq 1 the trace part of the solvent quadrupolarization is retained, so that $\mathbf{Q}(\mathbf{r})$ is the density of the quadrupole moment $\mathbf{q}$ evaluated over a small volume ΔV centered at $\mathbf{r}$

$$\mathbf{q} \equiv \frac{3}{2}\int^{\Delta V} d\mathbf{r}'\,\rho(\mathbf{r}+\mathbf{r}')\,\mathbf{r}'\mathbf{r}' \quad (2)$$

with the charge distribution ρ. Since $\mathbf{q}$ does not interact with itself, the corresponding contribution at the continuum level, viz., interaction of $\mathbf{Q}(\mathbf{r})$ and $\mathbf{Q}(\mathbf{r}')$ at $\mathbf{r} = \mathbf{r}'$ is excluded. This is denoted as the subscript 0^+ in eq 1. The subtraction of a similar self-interaction term for $\mathbf{P}_{el}$ is absorbed into χ_{el}. We note that the induced and permanent components of $\mathbf{q}$ (and thus $\mathbf{Q}$) are not distinguished in this continuum formulation of quadrupolar solvents in eq 1.

To simplify $\hat{H}$ in eq 1, we invoke the ansatz[35,36]

$$\mathbf{Q}(\mathbf{r}) = -3[\vec{\nabla}\vec{\nabla}\Lambda_Q(\mathbf{r}) + |\,f(\mathbf{r})]$$

$$\Lambda_Q(\mathbf{r}) = \frac{C_Q}{3\epsilon_\infty}\sum_{lm}\sqrt{\frac{4\pi}{2l+1}}S_l^{-1}\left[\frac{1}{r^{l+1}} + \kappa^{l+1}\beta_l k_l(\kappa r)\right]\lambda_{lm}Y_{lm}(\theta,\phi)$$

$$f(\mathbf{r}) = -\frac{16\pi\kappa^4 C_Q^2}{315\epsilon_\infty}\sum_{lm}\sqrt{\frac{4\pi}{2l+1}}S_l^{-1}\,\kappa^{l+1}\beta_l k_l(\kappa r)\,\lambda_{lm}Y_{lm}(\theta,\phi)$$

$$\kappa^2 C_Q = \frac{3}{32\pi}[(35-12\eta) + \sqrt{1225-280\eta+144\eta^2}];\quad \eta = \left(1-\frac{1}{\epsilon_\infty}\right)^{-1} \quad (3)$$

where | is the unit matrix, Y_{lm} are spherical harmonics with the origin at the center of the solute molecule and λ_{lm} represents the lm multipole component of a hypothetical solute charge distribution, with which the nonequilibrium $\mathbf{Q}$ under consideration would be in equilibrium. In eq 3, the κ factor measures the degree of screening of the solute electric field by $\mathbf{Q}$, β_l and S_l are dimensionless quantities defined as[35,36]

$$\beta_l = \left[\frac{l+1}{2l+1}k_{l+1}^d(\kappa a) + \frac{l}{2l+1}k_{l-1}^d(\kappa a) + \frac{16\pi}{105}\kappa^2 C_Q k_l(\kappa a)\right]^{-1}\frac{(l+1)(l+2)}{(\kappa a)^{l+3}}$$

$$S_l = 1 + \frac{l}{(2l+1)\epsilon_\infty}\left[1-\epsilon_\infty + \frac{4\pi}{3}(l-1)\kappa^2 C_Q(\kappa a)^l\beta_l\,k_{l-1}(\kappa a) + \left(1-\frac{16\pi}{35}\kappa^2 C_Q\right)(\kappa a)^{l+1}\beta_l\,k_l(\kappa a)\right] \quad (4)$$

and $k_l(z)$ and $k_l^d(z)$ are related to modified Bessel functions $K_n(z)$

$$k_l(z) = \sqrt{\frac{2}{\pi z}}K_{l+1/2}(z);\quad k_l^d(z) = \frac{l}{2}k_l(z) - k_{l+1}(z) \quad (5)$$

The lengthy expression in square brackets on the right-hand side of S_l arises from the cavity boundary.[35,36]

The relative time scales of the solute and solvent electronic motions play an important role in a variety of reactions in solution.[38] For a typical TICT system, the electronic coupling is small, so that the solvent electronic response is much faster than the solute electronic motions relevant to charge transfer.[14,18] In this regime, we can eliminate $\mathbf{P}_{el}$ adiabatically through $\delta\hat{H}/\delta\mathbf{P}_{el} = 0$ because it always follows the localized solute charge distributions.[38,39] We can then obtain $\hat{H}$ solely in terms of λ_{lm}[36]

$$\hat{H} = \hat{H}^0 - \frac{1}{2}\sum_{lm}R_\infty^{lm}\,\hat{\varphi}_{lm}^2 + \frac{1}{2}\sum_{lm}R_Q^{lm}\,(\lambda_{lm}^2 - 2\lambda_{lm}\hat{\varphi}_{lm}) \quad (6)$$

where $\hat{\varphi}_{lm}$ is the solute lm multipole operator

$$\hat{\varphi}_{lm} = \sqrt{\frac{4\pi}{2l+1}}\int d\mathbf{x}\,x^l\,Y_{lm}^*(\theta_x,\phi_x)\,\hat{\rho}_0(\mathbf{x}) \quad (7)$$

associated with its charge density operator $\hat{\rho}_0(\mathbf{x})$. The reaction field factors R_∞^{lm} and R_Q^{lm} in eq 6

$$R_\infty^{lm} = \frac{(l+1)(\epsilon_\infty-1)}{(l+1)\epsilon_\infty + l}\frac{1}{a^{2l+1}}$$

$$R_Q^{lm} = \frac{4\pi\,(l+1)(l+2)(2l+1)}{3\epsilon_\infty[(l+1)\epsilon_\infty + l]}\frac{\kappa^2 C_Q}{S_l}F_l(\kappa a)\frac{1}{a^{2l+1}} \quad (8)$$

characterize strengths of $\mathbf{P}_{el}$ and $\mathbf{Q}$ responses to the lm multipole moment, respectively. The $F_l(\kappa a)$ factor in R_Q^{lm} in eq 8

$$F_l(y) \equiv \frac{1}{y^2} + \frac{y^l}{2l+1}\beta_l(y)\,k_{l+1}(y) = \frac{\zeta\,(2l+1)y\,k_l(y) - l(l-1)k_{l-1}(y)}{y^2[(l+1)(l+2)k_{l+1}(y) + \zeta(2l+1)y\,k_l(y) - l(l-1)\,k_{l-1}(y)]}$$

$$\zeta \equiv 1 - \frac{16\pi}{105}\kappa^2 C_Q \quad (9)$$

gauges the short-range effect of the solute-quadrupole interactions, compared to solute-dipole interactions. The term involv-

ing R_∞^{lm} on the right-hand side of eq 6 describes the dispersion and polarization stabilizations of the solute through Coulombic interactions with $\mathbf{P}_{el}$.[39] The terms quadratic and linear in λ_{lm} represent, respectively, the self-energy of **Q** and its interaction with the solute, screened by $\mathbf{P}_{el}$.

3. Theory and Model for TICT

Isolated DMABN. Here we briefly explain the electronic description for DMABN employed in our study. In view of an excellent agreement between the previous analysis of ref 18 and EICT kinetics measurements in dipolar solvents, we use the two-state valence-bond (VB) description there without any modifications. To be specific, EICT of DMABN is described by two orthogonal diabatic VB states, a locally excited (LE) state $\psi_{le}(\theta)$ and a charge transfer (CT) state $\psi_{ct}(\theta)$, where θ is the above-mentioned twist angle between the amino group and phenyl ring. The DMABN wave function in solution is described as a linear combination of these two basis functions, with coefficients that vary with both θ and the solvent quadrupolarization configuration. In this VB representation, the vacuum electronic Hamiltonian $\hat{H}^0$ is given by

$$\hat{H}^0 = \begin{pmatrix} E_{le}^0(\theta) & -\beta(\theta) \\ -\beta(\theta) & E_{ct}^0(\theta) \end{pmatrix} \tag{10}$$

where E_{le}^0 and E_{ct}^0 are the vacuum diabatic energies for the LE and CT states, respectively, and β is the effective electronic coupling between the two. The solute electric field is assumed to be point-dipolar in either electronic configuration[14,18]

$$\hat{\vec{\mathcal{E}}}(\theta) = -\nabla\frac{\mathbf{r}\cdot\hat{p}}{r^3}; \quad \hat{p} = \begin{pmatrix} \vec{\mu}_{le}(\theta) & 0 \\ 0 & \vec{\mu}_{ct}(\theta) \end{pmatrix} \tag{11}$$

where $\hat{p}$ is the solute dipole operator and $\vec{\mu}_{le}$ and $\vec{\mu}_{ct}$ are the dipole moments associated with the LE and CT states, respectively.

In the model calculations, we employ the following vacuum diabatic energies (kcal mol^{-1}) and dipole moments (D) [ref 18]

$$E_{le}^0(\theta) = 13\sin^2\theta; \quad E_{ct}^0(\theta) = -1.5\sin^2\theta + 13$$

$$\mu_{le}(0) = 7; \quad \mu_{ct}(\theta) = 2\sin^2\theta + 13 \tag{12}$$

where both the LE and CT dipoles are parallel to the DMABN molecular axis. The parametric values in eq 12 were determined with the aid of existing ab initio quantum chemistry results[15] and experimental information on static electronic spectroscopy. As for the electronic coupling, we use[18]

$$\beta(\theta) = 1.8\cos^2\theta + 0.2 \text{ (kcal mol}^{-1}\text{)} \tag{13}$$

For further details on the DMABN model description and its parametrization, the reader is referred to refs 14 and 18.

Free Energy for EICT in Solution. We turn to DMABN in solution. With the point-dipole assumption above, $\hat{H}$ in quadrupolar solvents [eq 6] reduces to

$$\hat{H} = \hat{H}^0 - \frac{1}{2}R_\infty^{1m}\hat{p}^2 + \frac{1}{2}R_Q^{1m}(\vec{\lambda}^2 - 2\vec{\lambda}\cdot\hat{p}) \tag{14}$$

We emphasize that $\vec{\lambda}$ in eq 14 is the dipole moment of a hypothetical solute, with which nonequilibrium **Q** would be in equilibrium. Following the dipolar solvent case,[14,18] we introduce a dimensionless solvent coordinate s

$$\vec{\lambda} = s\{\vec{\mu}_{ct}(\theta = 0°) - \vec{\mu}_{le}(\theta = 0°)\} + \vec{\mu}_{le}(\theta = 0°) \tag{15}$$

(For example, $s = 0$ represents the **Q** configuration, which is equilibrated to the LE state charge distribution.) With eq 15, the effective Hamiltonian for DMABN in the two-state VB basis becomes

$$\hat{H} = \begin{pmatrix} G_{le}(\theta, s) & -\beta(\theta) \\ -\beta(\theta) & G_{ct}(\theta, s) \end{pmatrix} \tag{16}$$

where the diabatic free energies in solution vary with two reaction coordinates θ and s

$$G_{le}(\theta, s) = E_{le}^0 - \frac{1}{2}R_\infty^{1m}\mu_{le}^2(\theta) + \frac{1}{2}R_Q^{1m}\{s\mu_0 + \mu_1 + \mu_{le}(\theta)\}^2$$

$$G_{ct}(\theta, s) = E_{ct}^0 - \frac{1}{2}R_\infty^{1m}\mu_{ct}^2(\theta) + \frac{1}{2}R_Q^{1m}\{s\mu_0 + \mu_1 + \mu_{ct}(\theta)\}^2 \tag{17}$$

By diagonalizing $\hat{H}$, we obtain the two adiabatic excited electronic states in solution together with their free energies as a function of θ and s. In particular, the lower of the two, given by

$$G_{EICT}(\theta, s) = \frac{1}{2}[G_{le}(\theta, s) + G_{ct}(\theta, s)] - \frac{1}{2}[\{G_{le}(\theta, s) - G_{ct}(\theta, s)\}^2 + 4\beta^2(\theta)]^{1/2} \tag{18}$$

defines the electronic adiabatic free energy surface, upon which the solute torsional and collective solvent quadrupole motions occur after the initial photoexcitation from the ground state.

We note that except for the difference arising from the reaction field factors, the structures of eqs 14−18 are exactly the same as those derived previously for DMABN photoreactions in dipolar solvents.[14,18] Therefore, the kinetics analyses there, such as reaction free energetics, reaction paths, and rate constants, are directly transferable to the present case with only minor changes associated with R_∞^{1m} and R_Q^{1m}. Thus we will not present the technical details in our subsequent analysis of EICT in the quadrupolar solvents. The interested reader is referred to ref 14 for a more detailed description.

For numerical calculations, we need the cavity size a and **Q** susceptibility C_Q [cf. eqs 3, 4, 8, and 9]. We employed the same 4.3 Å for a as in ref 18. This value reproduces an ∼2.3 kcal mol^{-1} red shift of the DMABN charge transfer absorption band, observed experimentally when the solvent is changed from *n*-heptane to diethyl ether.[13,15] As for C_Q, we adjusted its value, such that it correctly reproduces experimentally observed Stokes shift[31] of coumarin 153 in each solvent.[35] With the static dielectric constant $\epsilon_0 = 2.3$, 2.4, and 2.2 for benzene, toluene and dioxane, respectively, this yields the corresponding C_Q values 3.56, 2.98, and 11.82 Å^2 at room temperature.

4. Results

The model calculation results are presented in Figure 1 and Table 1. We begin by considering effective polarity of quadrupolar solvents.

TABLE 1: Theoretical and Experimental Results for DMABN at Room Temperature[a,b]

solvent	ϵ_∞	ϵ_0	ϵ_{app}	C_Q	ω_s	$\Delta G^\ddagger$	ΔG_{rxn}	τ_{TST}	κ	τ_{exp}
benzene	2.24	2.3	4.59	3.56	9.4[c]	3.5	0.9	146	0.90	
toluene	2.23	2.4	4.32	2.98	17.7[c]	3.6	1.1	180	0.93	(60)[d]
dioxane	2.01	2.2	7.26	11.82	9.4[e]	2.6	0.7	35[e]	0.86	34[f]
					17.7[e]			31[e]	0.90	
acetonitrile[g]	1.81	35.9			8.3	1.5	−3.0	6.0	0.78	6[h], 4[i]

[a] Units for C_Q, ω, free energy and reaction times are Å^2, ps^{-1}, kcal mol^{-1}, and ps, respectively. [b] Reaction times are the inverse of the rate constants, e.g., $\tau_{TST} = k_{TST}^{-1}$. [c] Reference 32. [d] Extrapolation from low-temperature measurements between −50 °C and −94 °C [ref 13d]. [e] Estimations based on benzene and toluene solvent frequencies, respectively. [f] Reference 13a. [g] Calculated results are from ref 18. [h] Reference 19. [i] Reference 20.

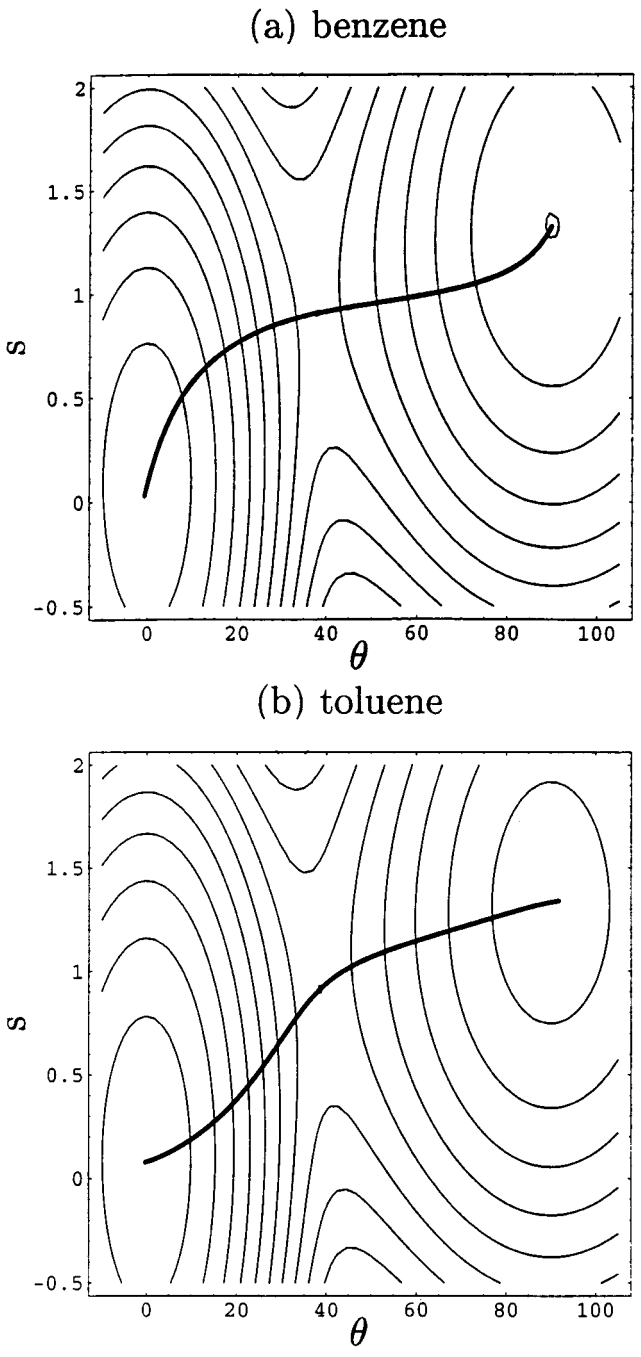

Figure 1. Adiabatic free energy surface $G_{EICT}(\theta, s)$ for DMABN in (a) benzene and (b) toluene. The free energy difference for two nearby contour lines is 0.35 kcal mol^{-1}. The SRP in each solvent is plotted as a thick solid line.

Apparent Dielectric Constant. In their recent continuum study, Jeon and Kim introduced an apparent dielectric constant ϵ_{app} for quadrupolar solvents[35]

$$\frac{2(\epsilon_{app}-1)}{2\epsilon_{app}+1}\frac{1}{a^3} \equiv R_\infty^{1m} + R_Q^{1m} \tag{19}$$

This is an effective dielectric constant, which takes into account the solvation effects of both $\mathbf{P}_{el}$ and $\mathbf{Q}$ of quadrupolar solvents [cf. eq 8]. From eqs 8 and 19, we see easily that ϵ_{app} varies with the cavity size. This is due to the fact that the quadrupolar fields are of shorter range than the dipolar fields. In Table 1, the results for ϵ_{app} in the presence of DMABN, i.e., with a = 4.3 Å, are compiled. It should be noticed that ϵ_{app} = 4.6, 4.3, and 7.3, respectively, for benzene, toluene, and dioxane are considerably larger than their ϵ_0 values, 2.3, 2.4, and 2.2. This means that the polarity of quadrupolar solvents measured as their capability of solvating dipolar solutes is significantly higher than the conventional scale based on their dielectric constant ϵ_0. This is because the contributions to solvation stabilization arising from the Coulombic interactions of the solutes with the solvent quadrupoles is completely neglected in the latter. Also in this context, dioxane is more "polar" and thus solvates charges and dipoles better than benzene and toluene. We note that various empirical solvent polarity scales,[40] such as $E_T(30)$ and π^*, show trends similar to what we have found here.

Reaction Free Energy Surface. In Figure 1, the excited-state reaction free energy surfaces G_{EICT} [eq 18] for DMABN in benzene and toluene are displayed as a function of θ and s. In each case, two local minima corresponding to the reactant and product states are separated by a barrier region with a saddle point, i.e., transition state.[41] The s and θ values for the two minima show that the reactant state ($s \approx 0$ and $\theta \approx 0°$) is essentially the LE state in planar geometry, while the product state ($s \approx 1.3$ and $\theta \approx 90°$) is mainly given by the CT state in perpendicular geometry. The location of the transition state is $\theta^\ddagger = 38°$ and $s^\ddagger = 0.90$ for benzene, 39° and 0.91 for toluene, and 33° and 0.87 for dioxane. Their respective barrier heights $\Delta G^\ddagger$ (viz., the free energy difference between the reactant and transition states) and free energies of reaction ΔG_{rxn} (i.e., free energy difference between the reactant and product states) are $\Delta G^\ddagger$ = 3.5, 3.6, and 2.6 kcal mol^{-1} and ΔG_{rxn} = 0.9, 1.1, and 0.7 kcal mol^{-1} [Table 1]. For comparison, EICT in highly dipolar acetonitrile is characterized by $\theta^\ddagger = 25°$, $s^\ddagger = 0.82$, and $\Delta G^\ddagger$ = 1.5 kcal mol^{-1}.[18]

Three points are important to make here. The first is that the qualitative features (and some quantitative aspects) of G_{EICT} and associated stable and unstable states in the quadrupolar solvents are nearly the same as those found previously for dipolar solvents.[14,18] This close similarity between the two different solvent classes clearly indicates that the solvent quadrupoles modulate the solution-phase free energetics in a significant way, analogous to the solvent dipoles. Second, because thermal energy k_BT is ∼0.6 kcal mol^{-1} at room temperature (k_B and T are Boltzmann's constant and temperature), charge-transfer

reactions for DMABN in the quadrupolar solvents studied here fall in the high barrier regime ($\Delta G^{\ddagger} \gtrsim 4k_BT$). Third, G_{EICT} in dioxane is characterized by an early transition state and a low barrier height, compared with benzene and toluene. Since the former is more polar than the latter two (in the ϵ_{app} context above), the CT state (and thus product state) is better stabilized in dioxane than in benzene and toluene. This makes the transition state character more reactant-state-like (Hammond postulate) and reduces the barrier height in dioxane. It should be pointed out that this trend with ϵ_{app} for the quadrupolar solvents is exactly the same as that with ϵ_0 for dipolar solvents.[14] Between benzene and toluene, their ϵ_{app} is nearly the same, and so are their reaction free energetics and transition state character.

Reaction Paths and Rate Constants. To understand the dynamical effects on EICT, we consider the solution-phase reaction path (SRP),[42] defined as a steepest descent path with zero kinetic energy from the transition state to the reactant and product states in the mass-weighted coordinate system[43]

$$\frac{I_\theta \, d\theta}{\partial G_{EICT}/\partial\theta} = \frac{m_s \, ds}{\partial G_{EICT}/\partial s} \tag{20}$$

Here I_θ and m_s are, respectively, the moment of inertia associated with solute torsional motions along θ and effective mass associated with solvent inertial dynamics along s. The latter motions, often accessible via ultrafast time-resolved spectroscopy,[3l,32] arise from non-dissipative, collective solvent quadrupole reorientations, i.e., inertial **Q** fluctuations, in our description. The values for the two mass factors are determined, so that the solute torsional frequency in a vacuum, $\omega_\theta \sim 14$ ps^{-1},[8,12] and solvent frequencies (viz., $\omega_s = 9.4$ and 17.7 ps^{-1} for benzene and toluene[32]) are well reproduced in our model description. The results for SRP are shown on the free energy surfaces in Figure 1. Even though their G_{EICT} are very similar, the SRP differs significantly between benzene and toluene due to the difference in ω_s. Specifically, for benzene whose inertial **Q** dynamics are slower than solute torsional motions, the solvent cannot keep up in the rapid passage over the barrier and it must extensively rearrange prior to that passage. Therefore its SRP in the barrier region is nearly in the twist coordinate, while it is mainly in the solvent coordinate near the reactant state. By contrast, for faster toluene, ω_s and ω_θ are nearly comparable, so that both s and θ are active participants throughout the entire course of reaction.

We proceed to the reaction rate. In the present study, we neglect the dissipative effects and determine the rate constant using the two-dimensional transition state theory (TST) expression[14]

$$k_{TST} = \frac{1}{2\pi} \frac{\omega_{\|}^R \omega_{\perp}^R}{\omega_{\perp}^{\ddagger}} \exp[-\Delta G^{\ddagger}/k_BT] \tag{21}$$

where the prefactor contains the frequencies in the reactant and transition state regions along (||) and transverse ($\perp$) to the SRP. Due to the lack of experimental information on its ω_s value, we considered two different cases for dioxane; i.e., k_{TST} evaluated with $\omega_s = 9.4$ and 17.7 ps^{-1}, corresponding to the benzene and toluene frequencies. The results for the reaction times $\tau_{TST} = k_{TST}^{-1}$ are summarized in Table 1. A general trend there is that the reaction becomes accelerated with increasing ϵ_{app}. This is mainly due to the enhancement in the solvation stabilization of the CT state, which in turn reduces the barrier height as mentioned above. Turning to individual solvents, our predictions for dioxane, $\tau_{TST} = 35$ and 31 ps, are in good accord with the experimental result, 34 ps [ref 13a]. As for toluene, the TST result, $\tau_{TST} = 180$ ps, is three times longer than the experimental estimate 60 ps, based on the low temperature measurements.[13d] While the discrepancy of this magnitude might look severe, it nonetheless corresponds to a mere $\sim k_BT$ difference in terms of $\Delta G^{\ddagger}$. Furthermore, considering the potential uncertainties involved in the extrapolation of the low T data, we think that the agreement between our analysis and experiments is also reasonable for toluene.

Finally, we consider the transmission coefficient κ, which measures the nonequilibrium solvation effect on the reaction rate; i.e., $k_{TST} = \kappa \, k_{ES}$, where k_{ES} is the rate constant determined under the assumption of equilibrium solvation.[14,18] For the quadrupolar solvents considered here, κ is found to be rather close to unity ($\sim$0.9 in Table 1). Because the barriers in these solvents are high as pointed out above, they are sharp with large curvature. Therefore, as the system crosses the barrier from the reactant side, it rapidly falls into the product well. As a result, it cannot easily recross the barrier back to the reactant region. This explains why the nonequilibrium solvation effect on rate constants in these solvents is lower than that in highly dipolar acetonitrile ($\kappa \sim 0.78$) with a smaller barrier.

5. Concluding Remarks

In this paper, we have studied excited-state intramolecular charge-transfer reactions of DMABN in polarizable, quadrupolar solvents. By combining the recent continuum theory of quadrupolar solvents[35−37] and the previous two-state TICT reaction formulation in dipolar solvents,[14,18] we investigated its reaction free energetics, reaction paths, and rate constants in benzene, toluene, and dioxane. We found that the basic features of the two-dimensional free energy surfaces in these solvents are nearly the same as those in highly dipolar solvents. We examined SRP on these surfaces with the aid of experimental information on ω_θ[8,12] and ω_s[32] and calculated the TST rate constants and transmission coefficients. It was found that our results for dioxane agree well with the measurements.[13a] However, the TST rate for toluene is about three times lower than the experimental estimate made via the extrapolation of low-temperature measurements.[13d]

In the present study, we have not considered the dissipation associated with solute torsional and solvent quadrupolarization dynamics. According to ref 18, dissipative dynamics make an important contribution to reaction kinetics for DMABN in hydroxylic solvents, such as methanol and ethanol. But it was also found there that the rate constants in the aprotic solvents are not strongly influenced. We thus believe that the current formulation with account of only nondissipative dynamics provides a reasonable description for DMABN photoreactions in quadrupolar solvents. Nevertheless, it will be worthwhile in the future to include dissipative dynamics and quantify its effects on excited-state intramolecular charge-transfer kinetics of DMABN and related TICT molecules.

Acknowledgment. This work was supported in part by NSF Grant No. CHE-0098062. We would like to thank Prof. Casey Hynes for useful comments. This article is dedicated to Prof. Noboru Mataga whose inspiring work has greatly advanced our understanding of charge transfer kinetics in solution.

References and Notes

(1) Lippert, E.; Lüder, W.; Moll, F.; Nagele, H.; Boos, H.; Prigge, H.; Siebold-Blankenstein, I. *Angew. Chem.* **1961**, *73*, 695. Lippert, E.; Lüder, W.; Boos, H. In *Advances in Molecular Spectroscopy*; Mangini, A., Ed.; Pergamon: Oxford, 1962.

(2) Grabowski, Z. R.; Rotkiewicz, K.; Siemiarczuk, A.; Cowley, D. J.; Baumann, W. *Nouv. J. Chim.* **1979**, *3*, 443. Lipiński, J.; Chojnacki, H.; Grabowski, Z. R.; Rotkiewicz, K. *Chem. Phys. Lett.* **1980**, *70*, 449.

(3) Rettig, W.; Wermuth, G.; Lippert, E. *Ber. Bunsen-Ges. Phys. Chem.* **1979**, *83*, 692. Rettig, W.; Lippert, E. *J. Mol. Structure (THEOCHEM)* **1980**, *61*, 17.

(4) Hicks, J.; Vandersall, M. T.; Babarogic, Z.; Eisenthal, K. *Chem. Phys. Lett.* **1985**, *116*, 18. Hicks, J.; Vandersall, M.; Sitzmann, E. V.; Eisenthal, K. *Chem. Phys. Lett.* **1987**, *135*, 413.

(5) Heisel, F.; Miehé, J. A. *Chem. Phys.* **1985**, *98*, 233. Heisel, F.; Miehé, J. A.; Martinho, J. M. G. *Chem. Phys.* **1985**, *98*, 243. Heisel, F.; Miehé, J. A. *Chem. Phys. Lett.* **1986**, *128*, 323.

(6) Su, S.-G.; Simon, J. D. *J. Chem. Phys.* **1988**, *89*, 908. *J. Phys. Chem.* **1989**, *93*, 753.

(7) Kajimoto, O.; Futakami, M.; Kobayashi, T.; Yamasaki, K. *J. Phys. Chem.* **1988**, *92*, 1347. Kajimoto, O.; Yokoyama, H.; Ooshima, Y.; Endo, Y. *Chem. Phys. Lett.* **1991**, *179*, 455.

(8) Warren, J. A.; Bernstein, E. R.; Seeman, J. I. *J. Chem. Phys.* **1988**, *88*, 871. Grassian, V. H.; Warren, J. A.; Bernstein, E. R.; Secor, H. V. *J. Chem. Phys.* **1989**, *90*, 3994.

(9) Moro, G. J.; Nordio, P. L.; Polimeno, A. *Mol. Phys.* **1989**, *68*, 1131. Polimeno, A.; Barbon, A.; Nordio, P. L.; Rettig, W. *J. Phys. Chem.* **1994**, *98*, 12158.

(10) Kato, S.; Amatatsu, Y. *J. Chem. Phys.* **1990**, *92*, 7241. Hayashi, S.; Ando, K.; Kato, S. *J. Phys. Chem.* **1995**, *99*, 955.

(11) Schenter, G. K.; Duke, C. B. *Chem. Phys. Lett.* **1991**, *176*, 563.

(12) Howell, R.; Petek, H.; Phillips, D.; Yoshihara, K. *Chem. Phys. Lett.* **1991**, *183*, 249.

(13) (a) Schuddeboom, W.; Jonker, S. A.; Warman, J. M.; Leinhos, U.; Kühnle, W.; Zachariasse, K. A. *J. Phys. Chem.* **1992**, *96*, 10809. (b) Zachariasse, K. A.; von der Haar, T.; Hebecker, A.; Leinhos, U.; Kühnle, W. *Pure Appl. Chem.* **1993**, *65*, 1745. (c) Zachariasse, K. A.; Grosby, M.; von der Haar, T.; Hebecker, A.; Il'ichev, Y. Y.; Morawski, O.; Rückert, I.; Kühnle, W. *J. Photochem. Photobiol. A* **1997**, *105*, 373. (d) Il'ichev, Y. Y.; Kühnle, W.; Zachariasse, K. A. *J. Phys. Chem. A* **1998**, *102*, 5670.

(14) (a) Fonseca, T.; Kim, H. J.; Hynes, J. T. *J. Mol. Liq.* **1994**, *60*, 161. (b) Fonseca, T.; Kim, H. J.; Hynes, J. T. *J. Photochem. Photobiol.* **1994**, *82*, 67.

(15) Serrano-Andrés, L.; Merchán, M.; Roos, B. O.; Lindh, R. *J. Am. Chem. Soc.* **1995**, *117*, 3189.

(16) Hynes, J. T. *Rev. Port. Quím.* **1995**, *2*, 12.

(17) Sobolewski, A. L.; Domcke, W. *Chem. Phys. Lett.* **1996**, *176*, 428.

(18) Kim, H. J.; Hynes, J. T. *J. Photochem. Photobiol. A* **1997**, *105*, 337.

(19) Changenet, P.; Plaza, P:; Martin, M. M.; Meyer, Y. H. *J. Phys. Chem. A* **1997**, *101*, 8186.

(20) Chudoba, C.; Kummrow, A.; Dreyer, J.; Stenger, J.; Nibbering, E. T. J.; Elsaesser, T.; Zachariasse, K. A. *Chem. Phys. Lett.* **1999**, *309*, 357.

(21) Dreyer, J.; Kummrow, A. *J. Am. Chem. Soc.* **2000**, *122*, 2577.

(22) Kwok, W. M.; Ma, C.; Phillips, D.; Matousek, P.; Parker, A. W.; Towrie, M. *J. Phys. Chem. A* **2000**, *104*, 4188.

(23) For reviews, see, e.g., Rettig, W. *Angew. Chem., Int. Ed. Engl.* **1986**, *25*, 971. Lippert, E.; Rettig, W.; Bonačić-Koutecký, V.; Heisel, F.; Miehé, A. *Adv. Chem. Phys.* **1987**, *68*, 1.

(24) Strictly speaking, toluene and dioxane are dipolar solvents because they have nonvanishing permanent dipole moments. However, due to their small magnitude (e.g., ~0.3 D for toluene), we expect that their contribution to solvation is nearly insignificant compared to the quadrupole moments. This is confirmed by their low dielectric constants, i.e., 2.4 and 2.2 for toluene and dioxane, which are typical values for nondipolar solvents. In this context, we will refer to them as quadrupolar solvents.

(25) Wasielewski, M. R.; Niemczyk, M. P.; Svec, W. A.; Pewitt, E. B. *J. Am. Chem. Soc.* **1985**, *107*, 1080.

(26) Harrison, R. J.; Pearce, B.; Beddard, G. S.; Cowan, J. A.; Sanders, J. K. M. *Chem. Phys.* **1987**, *116*, 429.

(27) Chatterjee, S.; Davis, P. D.; Gottschalk, P.; Kurz, M. E.; Sauerwein, B.; Yang, X.; Schuster, G. B. *J. Am. Chem. Soc.* **1990**, *112*, 6329.

(28) Asahi, T.; Ohkohchi, M.; Matsusaka, R.; Mataga, N.; Zhang, R. P.; Osuka, A.; Maruyama, K. *J. Am. Chem. Soc.* **1993**, *115*, 5665.

(29) (a) Read, I.; Napper, A.; Kaplan, R.; Zimmt, M. B.; Waldeck, D. H. *J. Am. Chem. Soc.* **1999**, *121*, 10976. (b) Read, I.; Napper, A.; Zimmt, M. B.; Waldeck, D. H. *J. Phys. Chem. A* **2000**, *104*, 9385.

(30) Berg, M. *Chem. Phys. Lett.* **1994**, *228*, 317.

(31) Reynolds, L.; Gardecki, J. A.; Frankland, S. J. V.; Horng, M. L.; Maroncelli, M. *J. Phys. Chem.* **1996**, *100*, 10337.

(32) Larsen, D. S.; Ohta, K.; Fleming, G. R. *J. Chem. Phys.* **1999**, *111*, 8970.

(33) Matyushov, D. V. *Chem. Phys.* **1993**, *174*, 199. Matyushov, D. V.; Schmid, R. *J. Chem. Phys.* **1995**, *103*, 2034.

(34) Perng, B.-C.; Newton, M. D.; Raineri, F. O.; Friedman, H. L. *J. Chem. Phys.* **1996**, *104*, 7153, 7177.

(35) Jeon, J.; Kim, H. J. *J. Solution Chem.* **2001**, *30*, 849.

(36) Jeon, J.; Kim, H. J., to be submitted to *J. Chem. Phys.*

(37) Jeon, J.; Kim, H. J. *J. Phys. Chem. A* **2000**, *104*, 9812.

(38) Kim, H. J.; Hynes, J. T. *J. Chem. Phys.* **1992**, *96*, 5088.

(39) Kim, H. J. *J. Chem. Phys.* **1996**, *105*, 6818.

(40) See, e.g., Reichardt, C. *Solvents and Solvent Effects in Organic Chemistry*, 2nd ed.; Verlag Chemie: Weinheim, 1988.

(41) Though not shown here, the structures of the reaction free energy surface for dioxane are similar.

(42) Lee, S.; Hynes, J. T. *J. Chem. Phys.* **1988**, *88*, 6853.

(43) Fukui, K. *J. Phys. Chem.* **1970**, *74*, 4161. Fukui, K. *Acc. Chem. Res.* **1981**, *14*, 363.